

Ablation of B7-H3 but Not B7-H4 Results in Highly Increased Tumor Burden in a Murine Model of Spontaneous Prostate Cancer

Katharina Kreymborg¹, Stefan Haak^{2,3}, Rajmohan Murali^{4,5}, Joyce Wei⁶, Rebecca Waitz¹, Georg Gasteiger¹, Peter A. Savage⁷, Marcel R. M. van den Brink⁸, and James P. Allison^{1,6}

Abstract

The costimulatory molecules B7-H3 and B7-H4 are overexpressed in a variety of human tumors and have been hypothesized as possible biomarkers and immunotherapeutic targets. Despite this potential, the predominating uncertainty about their functional implication in tumor–host interaction

hampers their evaluation as a target for cancer therapy. By means of a highly physiologic, spontaneous tumor model in mice, we establish a causal link between B7-H3 and host tumor control and found B7-H4 to be redundant. *Cancer Immunol Res*; 3(8); 849–54. ©2015 AACR.

Introduction

The immune system can recognize spontaneous malignancies and mediate their elimination (1, 2), which is greatly influenced by the tumor microenvironment. Cancer immunotherapy aims at promoting the activation of immune effector mechanisms or blocking inhibitory pathways to elicit and sustain an endogenous antitumor response. In this regard, cosignaling molecules as accessory modulators of T-cell responses are of particular interest as they are determining factors between tolerance and immunity (3). Their targeting for cancer immunotherapy has gained conceptual validation in recent years, as several efforts have shown success in phase II and phase III clinical trials or received FDA approval as standard-of-care therapies for the treatment of cancer patients (4). A prerequisite for improving clinical benefit from combination therapies and for the development of new strategies is a clear understanding of the factors

critically involved in shaping the antitumor immune response. In addition, identification of biomarkers is vital for the rational choice of combinatorial treatments and the advancement of individualized immunotherapy.

With these objectives, we focused on the cosignaling molecules B7-H3 and B7-H4 in a stringent genetic study. Both molecules have been related to immune-modulatory processes in the tumor microenvironment, as they are overexpressed on a variety of human tumors. Although B7-H4 expression has been correlated with poor clinical outcome, studies investigating associations of B7-H3 expression with survival have shown conflicting results (5). Furthermore, the receptor(s) for B7-H3 or B7-H4 have not been identified conclusively, and the physiologic role of B7-H3 particularly is elusive, as both immune-stimulatory and immune-inhibitory capacities have been demonstrated *in vitro* and *in vivo* (6, 7).

To causally determine the function and relevance of B7-H3 and B7-H4 in cancer progression, we employed the TRAMP (transgenic adenocarcinoma of the mouse prostate) model, in which male mice develop spontaneous prostate cancer with a history similar to that of the human disease (8) and in which we were able to genetically ablate B7-H3 or B7-H4.

Materials and Methods

Mice

TRAMP⁺ mice were a gift from N. Greenberg (Fred Hutchinson Cancer Research Center, Seattle, WA), maintained in the hemizygous state, and crossed with B7-H3^{-/-} or B7-H4^{-/-} mice. Male TRAMP⁺ and TRAMP⁻ littermate control mice of wild-type (WT), B7-H4^{-/-}, and B7-H4^{-/-} breedings were used for analysis at indicated time points. B7-H3^{-/-} mice were a gift from T. Mak (University of Toronto, Toronto, ON, Canada). The generation of B7-H4^{-/-} was previously described (9). All breedings were maintained on the C57BL/6 background, and the full C57BL/6 background of all strains was confirmed by analysis of 1,449 SNPs. C57BL/6 mice were purchased from The Jackson Laboratory, and CD45.1⁺ B6.SJL mice were from Taconic. All mice were bred and

¹Program in Immunology, Howard Hughes Medical Institute, and Ludwig Center for Cancer Immunotherapy, Memorial Sloan Kettering Cancer Center, New York, New York. ²Columbia University Medical Center, New York, New York. ³Centre of Allergy and Environment (ZAUM), Technical University and Helmholtz Centre Munich, Munich, Germany. ⁴Department of Pathology, Memorial Sloan Kettering Cancer Center, New York, New York. ⁵Human Oncology and Pathogenesis Program, Memorial Sloan Kettering Cancer Center, New York, New York. ⁶Department of Immunology, The University of Texas MD Anderson Cancer Center, Houston, Texas. ⁷Department of Pathology, University of Chicago, Chicago, Illinois. ⁸Department of Immunology and Medicine, Memorial Sloan Kettering Cancer Center, New York, New York.

Note: Supplementary data for this article are available at Cancer Immunology Research Online (<http://cancerimmunolres.aacrjournals.org/>).

K. Kreymborg and S. Haak contributed equally to this article.

Corresponding Author: James P. Allison, The University of Texas MD Anderson Cancer Center, 1515 Holcombe Boulevard, Box 470, Z-1560, Houston, TX 77030. Phone: 646-888-2332; Fax: 646-422-0470; E-mail: JAllison@mdanderson.org

doi: 10.1158/2326-6066.CIR-15-0100

©2015 American Association for Cancer Research.

Kreymborg et al.

maintained under specific pathogen-free conditions, and animal experimentation was conducted in accordance with institutional guidelines.

RNA preparation and real-time PCR

RNA was isolated from homogenized tissue using the RNeasy Kit (Qiagen). RNA (1–5 µg) was reverse-transcribed using Ready-To-Go You-Prime First-Strand Beads (GE Healthcare). Quantitative PCR was performed on a real-time PCR system (Applied Biosystems/7500) using TaqMan primer/probe gene expression assays for each gene analyzed (Applied Biosystems). GAPDH was used as the endogenous control. Relative changes in gene expression were calculated using the $\Delta\Delta C_t$ method. Focused qPCR arrays (PAMM-135Z, PAMM-074Z) were purchased from Qiagen.

Tumor evaluation and histopathology

Mice were weighed prior to euthanization by CO₂ inhalation at indicated time points (between 6 and 36 weeks of age). The whole urogenital tract, as well as the anterior, ventral, and dorsolateral prostate lobes were dissected and individually weighed. All weights were normalized to whole body weight. Dorsolateral prostate lobes were fixed in 10% buffered neutral formalin and embedded in paraffin. Tissue sections (5-µm-thick; ≥8 spaced cuts per mouse) were routinely stained with hematoxylin and eosin and microscopically examined.

Isolation of cells from mouse prostate and lymph nodes

The dorsolateral prostate lobes were dissected, mechanically disrupted and digested using DNase (Sigma-Aldrich) and liberase (Roche) for 30 minutes at 37°C in complete RPMI media, and filtered through a 70-µm cell strainer (BD Biosciences). Lymphocytes were enriched using centrifugation over Histopaque-1119 (Sigma). Tumor cells for *in vitro* culture were depleted of CD45⁺-infiltrating cells by FACS, 10⁴ cells were cultured in 200 µL of a 4 mg collagen matrix (Matrigel; BD Biosciences) for 5 days, released by incubation in Dispase (BD Biosciences) for 2 hours at 37°C, and counted. Draining (periaortic) and nondraining (brachial) lymph nodes (LN) were dissected, mechanically disrupted, and filtered through a 70-µm cell strainer (BD Biosciences).

Flow cytometry

Fluorescently labeled antibodies were purchased from eBioscience or BD Biosciences. Dead cells were stained using the fixable aqua dead cell stain Kit (Molecular Probes); surface markers were stained in the presence of 2.4G2 mAb (MSKCC Monoclonal Antibody Core Facility) to block FcγR binding. The intracellular staining Kit from eBioscience was used after stimulation with 50 ng/mL phorbol 12-myristate 13-acetate (PMA; Sigma), 1 µmol/L ionomycin (Sigma), and GolgiStop (BD Biosciences) in complete RPMI at 37°C for 4 hours. Anti-B7-H3-PE and anti-B7-H4-PE fluorescence intensity was amplified using the Faser Kit (Miltenyi Biotec). Samples were acquired using a LSR II flow cytometer (Becton Dickinson) and analyzed using FlowJo software (Tree Star). The absolute number of cells per tumor sample was quantified using fluorescent microbeads (Life Technologies) and normalized to a known sample volume, which was then normalized to tumor wet weight.

Immunohistochemistry

Tissue was fixed in 10% buffered neutral formalin and embedded in paraffin. Tissue sections (5-µm-thick) were stained with anti-Ki67 (MSKCC Pathology Core Facility), and the Ki-67 index

(percentage of cells showing nuclear expression of Ki-67) was assessed using a light microscope.

Bone marrow chimeras

Bone marrow chimeras were generated using bone marrow from the femurs of CD45.1⁺B6.SJL or CD45.2⁺B7-H3^{-/-} mice. Six- to 7-week-old recipient CD45.2⁺TRAMP⁺ B7-H3^{-/-}, CD45.2⁺TRAMP⁺, or TRAMP⁻ controls were lethally irradiated, exposing them to two, 24-hour spaced doses of 600 Gy and reconstituted with 5 × 10⁶ bone marrow cells. Twelve weeks later, mice were bled to confirm chimerism. LNs, urogenital tracts, and individual prostate lobes were harvested and analyzed when mice were 30 weeks old.

Proliferation assays

T cells were purified from LN cell suspensions by magnetic cell sorting with CD90 Microbeads (Miltenyi Biotec). Cells were cultured for 48 hours in round-bottom plates coated over night at 4°C with 0.5 µg/mL anti-CD3 and either B7-H3 Ig or control Ig at indicated concentrations. Proliferation was monitored by the addition of ³H-methyl-thymidine (1 µCi/well) for the last 24 hours of culture. Cells were harvested onto glass-fiber filters using a Tomtec harvester, and filters were counted using a MicroBeta scintillation counter (Perkin-Elmer).

Cytotoxicity assays

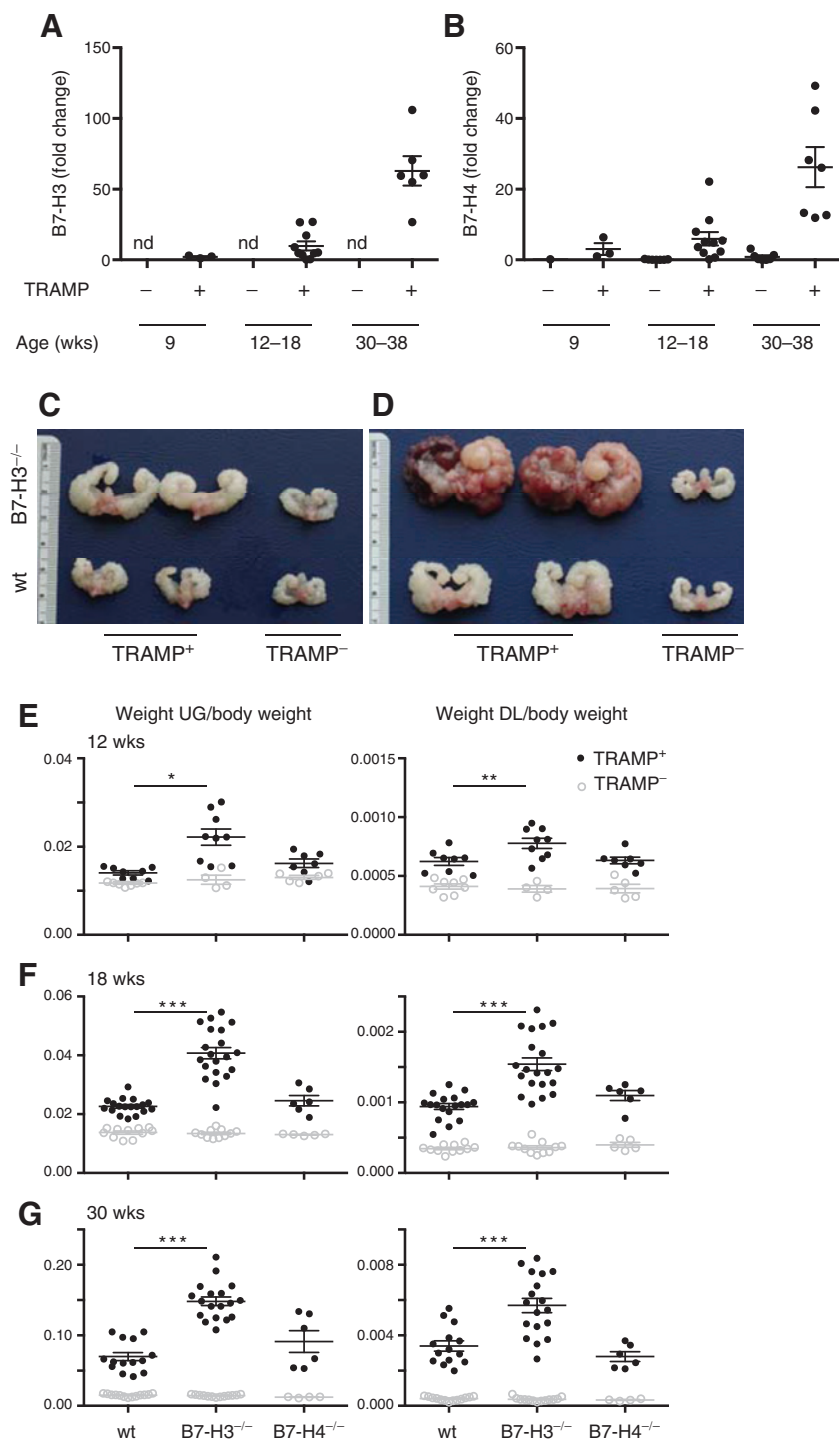
RMA and RMA-S cells were obtained from Dr. Ljunggren (Karolinska Institute, Stockholm, Sweden). All cell lines were tested and validated to be mycoplasma free; no genomic authentication was performed. RMA and RMA-S cells were transfected with B7-H3, irrelevant protein (Thy1.1), or empty vector using the murine stem cell virus retroviral expression system. Cells expressing high levels of the transfected proteins were sorted by FACS. For measurement of *in vivo* natural killer (NK)-cell-mediated cytotoxicity, RMA and RMA-S cells were labeled with different concentrations of cfse or eFlour670 (eBioscience) and injected i.v. into naïve C57BL/6 mice or mice that had received 100 µg of depleting anti-NK1.1 antibody (PK-136; BioXCell) 48 hours earlier. Labeled cells were recovered from lungs 4 hours after injection. Percent cytotoxicity was determined as 100 – (100 × (%RMA-S/%RMA))/(%RMA-s/%RMA in NK-cell-depleted mice). For *in vitro* CD8⁺ T-cell-mediated cytotoxicity, SPASTc mice were used, which express a T-cell receptor specific for the TRAMP-C2 tumor antigen SPAS-1-derived H8 peptide (10). SPASTc splenocytes were activated for 6 days with H8 peptide and 100 U/mL of recombinant human IL2 (PeproTech), subsequently used as effectors and H8-pulsed RMA cells as targets in a lactate dehydrogenase (LDH) release Cytotox-One Assay (Promega) following the manufacturer's instructions. Percent cytotoxicity was determined as 100 × ((experimental – effectors alone)/(maximum LDH release – effectors alone)).

Statistical analysis

Analysis was performed using Graph Prism software (GraphPad). Where data sets were normally distributed, *t* tests were performed.

Results and Discussion

We analyzed the expression of B7-H3 and B7-H4 mRNA and protein in primary TRAMP⁺ tumors *ex vivo* by qPCR and flow

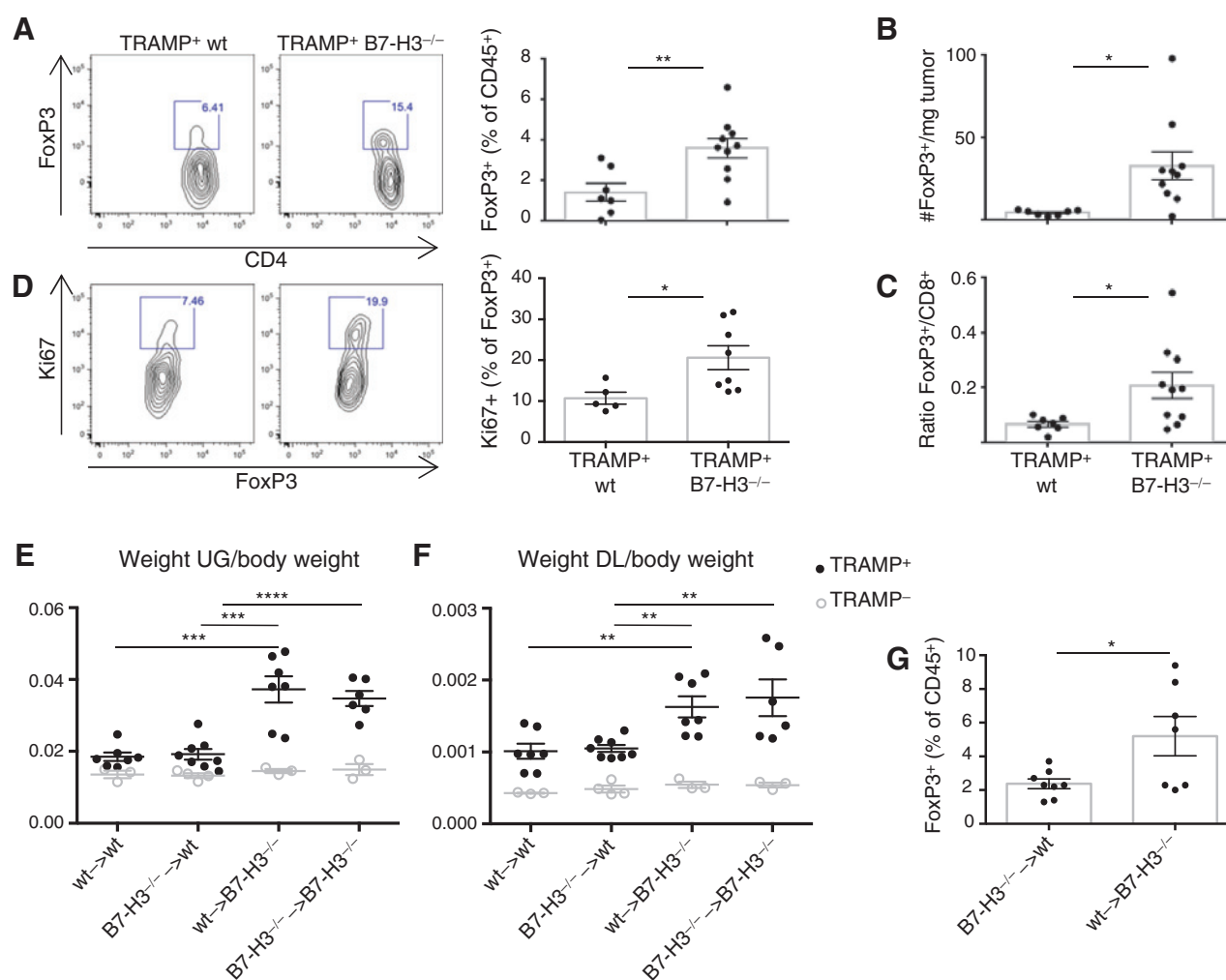
**Figure 1.**

Greatly increased growth of murine prostate tumors in the absence of B7-H3. A, B7-H3 and B, B7-H4 mRNA expression in the DL prostate lobes of male TRAMP⁺ or age-matched TRAMP⁻ littermate control mice at indicated time points measured by qPCR and calculated by $2^{-(\Delta\Delta Ct)} \pm \text{SEM}$ ($n \geq 3$ per group). C, representative images of UG of 18-week- and D, 30-week-old TRAMP⁺WT, TRAMP⁺B7-H3^{-/-}, and age-matched TRAMP⁻WT or TRAMP⁻B7-H3^{-/-} littermate control mice, respectively. E, masses of UG and DL prostates of TRAMP⁺WT, TRAMP⁺B7-H3^{-/-}, TRAMP⁺B7-H4^{-/-}, and corresponding TRAMP⁻WT, TRAMP⁻B7-H3^{-/-}, or TRAMP⁻B7-H4^{-/-} littermate control mice, respectively, evaluated at 12 weeks, (F) 18 weeks, and (G) 30 weeks of age and normalized to whole body weight \pm SEM (TRAMP⁺WT: $n = 39$; TRAMP⁺B7-H3^{-/-}: $n = 48$; TRAMP⁺B7-H4^{-/-}: $n = 21$; TRAMP⁻WT: $n = 33$; TRAMP⁻B7-H3^{-/-}: $n = 28$; TRAMP⁻B7-H4^{-/-}: $n = 14$). Unpaired t test. *, $P < 0.05$; **, $P < 0.01$; and ***, $P < 0.001$.

cytometry, respectively. Reflecting the situation in human prostate cancer (11), expression of both molecules was markedly elevated in tumors and the expression increased with cancer progression (Fig. 1A and B and Supplementary Fig. S1). To determine the impact of B7-H3 and B7-H4 on tumor growth, we analyzed TRAMP⁺ tumor progression in mice deficient in either molecule at different stages of tumor development. Tumor burden was assessed by weight of the entire urogenital tract (UG) and the

dissected dorsolateral (DL) prostate lobes, as well as by histologic analysis. Strikingly, mice lacking B7-H3 showed dramatically increased tumor sizes (Fig. 1C-G). Tumor development in TRAMP mice starts with puberty at week 5 to 6. The aggravated tumor burden observed in TRAMP⁺B7H3^{-/-} mice was detectable as early as 12 weeks of age and increased over time. Histopathologic analysis revealed a higher abundance of neoplastic epithelium and increased atypia in TRAMP⁺B7H3^{-/-} mice compared

Kreymborg et al.

**Figure 2.**

A, percentages of tumor-infiltrating FoxP3⁺ cells. B, total FoxP3⁺ cell counts per mg of tumor. C, ratio of FoxP3⁺ to CD8⁺ T cells; and D, Ki67⁺FoxP3⁺ cells isolated from TRAMP⁺wt and TRAMP⁺B7-H3^{-/-} tumors at 18 weeks of age and analyzed by flow cytometry \pm SEM ($n \geq 5$). (E), masses of UG and (F) DL prostates of indicated bone marrow chimeric TRAMP⁺wt, TRAMP⁺B7-H3^{-/-} and corresponding TRAMP⁻ control mice evaluated at 30 weeks of age and normalized to whole body weight \pm SEM. (TRAMP⁺, $n \geq 6$) G, Percentages of tumor-infiltrating FoxP3⁺ cells isolated from indicated bone marrow chimeric TRAMP⁺ mice at 30 weeks of age. Unpaired t test. *, $P < 0.05$; **, $P < 0.01$; ***, $P < 0.001$; ****, $P < 0.0001$.

with TRAMP⁺WT mice (Supplementary Fig. S2). In contrast with the drastic impact of B7-H3 expression on tumor development, tumor progression was found to be independent of B7-H4 (Fig. 1E-G). TRAMP tumors develop due to androgen-driven expression of the complete SV40 T antigen under the control of the probasin promoter (8, 12). To address potential interference by differences in levels of testosterone or androgen receptor expression that could account for the phenotype, we analyzed their levels in WT and B7-H3^{-/-} mice and found them to be comparable (Supplementary Fig. S3). Recently, a nonimmunologic, tumor cell-autonomous function of B7-H3 has been described using siRNA-mediated downregulation of B7-H3 in cancer cell lines (13). To test whether B7-H3 influences proliferation of primary TRAMP⁺ tumor cells in a cell-intrinsic manner, we first evaluated their expression of the cell cycle marker Ki67. We found it to be expressed at comparable levels in tumor cells extracted from early as well as late-stage TRAMP⁺B7-H3^{-/-} tumors and

corresponding WT controls (Supplementary Fig. S4). Secondly, we isolated primary tumor cells from TRAMP⁺WT and TRAMP⁺B7H3^{-/-} mice, expanded them in a three-dimensional collagen matrix *ex vivo*, and confirmed equal rates of proliferation (Supplementary Fig. S4). Results from both assays suggest a cell-extrinsic mode of action for B7-H3 during tumor development. To test whether this effect is immune mediated, we characterized the tumor microenvironment by assessing mRNA expression of genes implicated in immune responses within the DL prostates of 12-, 18-, and 30-week-old TRAMP⁺WT and TRAMP⁺B7-H3^{-/-} mice. Consistently, IL10 and TGF β transcripts were markedly elevated in the tumors of 30-week-old TRAMP⁺B7-H3^{-/-} mice, whereas IFN γ transcripts were less abundant in B7-H3^{-/-} tumors (Supplementary Fig. S5). These data adumbrate an altered and potentially more suppressive immune environment in the absence of B7-H3. Correspondingly, we found a slight trend toward a decrease in the relevant effector cytokine expression by

B7-H3^{-/-} tumor-infiltrating CD8⁺ T cells as well as NK cells (Supplementary Fig. S5). Previous studies have reported B7-H3 to either promote or inhibit T-cell proliferation and effector responses in various assays (14). In our *in vivo* setting, B7-H3 did not have a prominent direct effect on effector CD4⁺ or CD8⁺ T-cell proliferation or CD8⁺ T-cell- or NK-cell-mediated cytotoxicity as tested by ³H-thymidine incorporation in the presence of plate-bound B7-H3Ig or specific lysis of B7-H3-transfected target cells, respectively (Supplementary Fig. S6). Conclusively, searching for the primary difference on the cellular effector level, we observed a significant accumulation of FoxP3⁺ T cells (Treg) in B7-H3^{-/-} tumors (Fig. 2A–C), while at the same time percentages of Tregs in non-draining and tumor-draining LNs were the same in TRAMP⁺WT and TRAMP⁺B7-H3^{-/-} mice (Supplementary Fig. S7). An overview of other tumor-infiltrating cell populations is given in Supplementary Fig. S8. Lack of B7-H3 led to an increased proliferative activity of Tregs (Fig. 2D). Taken together, our results demonstrate an effective immune regulation due to the expression of B7-H3, but not the expression of B7-H4, on the local tumor microenvironment.

B7-H3 is predominantly expressed in nonhematopoietic tissue (6), but its expression has also been detected in activated lymphocytes *in vitro* (15), activated macrophages (16), and endothelial cells of the tumor-associated vasculature (17). We confirm the notion of a hematopoietic expression of B7-H3 by *ex vivo* cytometric analysis (Supplementary Fig. S9), raising the question of whether it is B7-H3 expression on tumor tissue or on tumor-infiltrating lymphocytes that accounts for the phenotype of the altered tumor burden. To address this question, we generated bone marrow chimeric TRAMP⁺ mice in which B7-H3 was absent from the mostly radiosensitive hematopoietic compartment (B7-H3^{-/-}→TRAMP⁺WT) or the radioresistant tissues only (WT→TRAMP⁺B7-H3^{-/-}) and subsequently assessed tumor progression. Although chimeric B7-H3^{-/-}→TRAMP⁺WT tumors were comparable with solely WT (WT→TRAMP⁺WT) controls, chimeric WT→TRAMP⁺B7-H3^{-/-} tumors were significantly larger and comparable with B7-H3^{-/-} (B7-H3^{-/-}→TRAMP⁺B7-H3^{-/-}) tumors (Fig. 2E and F). Notably, the percentages of FoxP3⁺ cells were significantly increased only in WT→TRAMP⁺B7-H3^{-/-}, but not in B7-H3^{-/-}→TRAMP⁺WT tumors (Fig. 2G), reflecting the phenotype in nonchimeric B7-H3^{-/-} and WT tumors, respectively. Therefore, the absence of B7-H3 in radioresistant tissue, most likely in the tumor, and not cells of hematopoietic origin accounts for a local increase in Treg numbers and the elevated tumor burden.

In summary, this genetic study affirms the potential of both B7-H3 and B7-H4 to serve as biomarkers in prostate cancer, but clearly shows a hereof-detached function of immune regulation. The vast impact specifically of B7-H3 on solid tumor growth in the applied model of tumorigenesis highlights its potential in shaping the tumor microenvironment and fosters the notion of B7-H3 as a valuable immunomodulatory target in cancer immunotherapy. There is a growing body of evidence describing a direct association of an increased accumulation of FoxP3⁺ cells in the microenvi-

ronment of human solid tumors and an adverse clinical outcome (18). Immune modulation by interfering local Treg activity also significantly contributes to the success of therapeutic interventions targeting cosignaling molecules in tumor immunotherapy (19).

There are burning questions arising from this substantive evidence of exacerbated tumor burden in the absence of B7-H3 as well as from other recent studies about the differing functions attributed to B7-H3, particularly in view of the ongoing clinical evaluation of an anti-B7-H3 antibody targeting tumor cells (MGA271; MacroGenics). Although the full mechanistic underpinnings of the impact of B7-H3 on tumor development remain to be established, it is tempting to conjecture on the basis of our findings that B7-H3 acts, directly or indirectly, in an inhibitory manner upon Tregs, which could result in an impaired antitumor immune response in its absence. In order to verify this hypothesis, the foremost goal is to find all types of receptors for B7-H3, along with their expression profile, and to study the immediate downstream responses at the cellular and molecular level.

Disclosure of Potential Conflicts of Interest

M.R.M. van den Brink reports receiving speakers bureau honoraria from Merck and is a consultant/advisory board member for Boehringer Ingelheim, Merck, and Novartis. J.P. Allison has ownership interest (including patents) in Bristol-Myers Squibb and Jounce Therapeutics and is a consultant/advisory board member for Jounce Therapeutics. No potential conflicts of interest were disclosed by the other authors.

Authors' Contributions

Conception and design: K. Kreymborg, S. Haak, P.A. Savage
Development of methodology: K. Kreymborg, R. Waitz, P.A. Savage
Acquisition of data (provided animals, acquired and managed patients, provided facilities, etc.): K. Kreymborg, S. Haak, J. Wei, R. Waitz, G. Gasteiger
Analysis and interpretation of data (e.g., statistical analysis, biostatistics, computational analysis): K. Kreymborg, S. Haak, R. Murali, J. Wei, R. Waitz, G. Gasteiger, J.P. Allison
Writing, review, and/or revision of the manuscript: K. Kreymborg, S. Haak, R. Murali, J. Wei, R. Waitz, J.P. Allison
Administrative, technical, or material support (i.e., reporting or organizing data, constructing databases): K. Kreymborg, S. Haak, M.R.M. van den Brink, J.P. Allison
Study supervision: K. Kreymborg, J.P. Allison
Other (pathology review): R. Murali

Acknowledgments

The authors thank Jacqueline Candelier (Laboratory of Comparative Pathology, MSKCC) for technical assistance and Emily Corse for critical comments and scientific discussion.

Grant Support

This work was supported by the Howard Hughes Medical Institute (to J.P. Allison), the cancer research institute (to K. Kreymborg and G. Gasteiger), and the Swiss National Science Foundation (to S. Haak).

Received April 17, 2015; revised June 7, 2015; accepted June 9, 2015; published OnlineFirst June 29, 2015.

References

- Kaplan DH, Shankaran V, Dighe AS, Stockert E, Aguet M, Old LJ, et al. Demonstration of an interferon gamma-dependent tumor surveillance system in immunocompetent mice. *Proc Natl Acad Sci U S A* 1998;95:7556–61.
- Shankaran V, Ikeda H, Bruce AT, White JM, Swanson PE, Old LJ, et al. IFN γ and lymphocytes prevent primary tumour development and shape tumour immunogenicity. *Nature* 2001;410:1107–11.

Kreymborg et al.

3. Peggs KS, Quezada SA, Allison JP. Cancer immunotherapy: co-stimulatory agonists and co-inhibitory antagonists. *Clin Exp Immunol* 2009;157:9–19.
4. Hodi FS, O'Day SJ, McDermott DF, Weber RW, Sosman JA, Haanen JB, et al. Improved survival with ipilimumab in patients with metastatic melanoma. *N Engl J Med* 2010;363:711–23.
5. Loos M, Hedderich DM, Friess H, Kleeff J. B7-h3 and its role in antitumor immunity. *Clin Dev Immunol* 2010;2010:683875.
6. Chapoval AI, Ni J, Lau JS, Wilcox RA, Flies DB, Liu D, et al. B7-H3: a costimulatory molecule for T cell activation and IFN-gamma production. *Nat Immunol* 2001;2:269–74.
7. Suh WK, Gajewska BU, Okada H, Gronski MA, Bertram EM, Dawicki W, et al. The B7 family member B7-H3 preferentially down-regulates T helper type 1-mediated immune responses. *Nat Immunol* 2003;4:899–906.
8. Greenberg NM, DeMayo F, Finegold MJ, Medina D, Tilley WD, Aspinall JO, et al. Prostate cancer in a transgenic mouse. *Proc Natl Acad Sci U S A* 1995;92:3439–43.
9. Wei J, Loke P, Zang X, Allison JP. Tissue-specific expression of B7x protects from CD4 T cell-mediated autoimmunity. *J Exp Med* 2011;208:1683–94.
10. Waitz R. Enhancement of T cell responses through Ctl4-4 blockade combination therapy in a mouse model of prostate cancer. Proquest: Umi Dissertation Publishing; 2011.
11. Zang X, Thompson RH, Al Ahmadie HA, Serio AM, Reuter VE, Eastham JA, et al. B7-H3 and B7x are highly expressed in human prostate cancer and associated with disease spread and poor outcome. *Proc Natl Acad Sci U S A* 2007;104:19458–63.
12. Ittmann M, Huang J, Radaelli E, Martin P, Signoretti S, Sullivan R, et al. Animal models of human prostate cancer: the consensus report of the New York meeting of the Mouse Models of Human Cancers Consortium Prostate Pathology Committee. *Cancer Res* 2013;73:2718–36.
13. Tekle C, Nygren MK, Chen YW, Dybsjord I, Nesland JM, Maelandsmo GM, et al. B7-H3 contributes to the metastatic capacity of melanoma cells by modulation of known metastasis-associated genes. *Int J Cancer* 2012;130:2282–90.
14. Wang L, Kang FB, Shan BE. B7-H3-mediated tumor immunology: friend or foe? *Int J Cancer* 2014;134:2764–71.
15. Steinberger P, Majdic O, Derdak SV, Pfistershammer K, Kirchberger S, Klauser C, et al. Molecular characterization of human 4lg-B7-H3, a member of the B7 family with four Ig-like domains. *J Immunol* 2004;172:2352–9.
16. Chen C, Shen Y, Qu QX, Chen XQ, Zhang XG, Huang JA. Induced expression of B7-H3 on the lung cancer cells and macrophages suppresses T-cell mediating anti-tumor immune response. *Exp Cell Res* 2013;319:96–102.
17. Kraan J, van den BP, Verhoef C, Grunhagen DJ, Taal W, Gratama JW, et al. Endothelial CD276 (B7-H3) expression is increased in human malignancies and distinguishes between normal and tumour-derived circulating endothelial cells. *Br J Cancer* 2014;111:149–56.
18. Curiel TJ, Coukos G, Zou L, Alvarez X, Cheng P, Mottram P, et al. Specific recruitment of regulatory T cells in ovarian carcinoma fosters immune privilege and predicts reduced survival. *Nat Med* 2004;10:942–9.
19. Nishikawa H, Sakaguchi S. Regulatory T cells in cancer immunotherapy. *Curr Opin Immunol* 2014;27:1–7.

Cancer Immunology Research

Ablation of B7-H3 but Not B7-H4 Results in Highly Increased Tumor Burden in a Murine Model of Spontaneous Prostate Cancer

Katharina Kreymborg, Stefan Haak, Rajmohan Murali, et al.

Cancer Immunol Res 2015;3:849-854. Published OnlineFirst June 29, 2015.

Updated version Access the most recent version of this article at:
doi:[10.1158/2326-6066.CIR-15-0100](https://doi.org/10.1158/2326-6066.CIR-15-0100)

Supplementary Material Access the most recent supplemental material at:
<http://cancerimmunolres.aacrjournals.org/content/suppl/2015/06/27/2326-6066.CIR-15-0100.DC1>

Cited articles This article cites 18 articles, 6 of which you can access for free at:
<http://cancerimmunolres.aacrjournals.org/content/3/8/849.full#ref-list-1>

Citing articles This article has been cited by 1 HighWire-hosted articles. Access the articles at:
<http://cancerimmunolres.aacrjournals.org/content/3/8/849.full#related-urls>

E-mail alerts [Sign up to receive free email-alerts](#) related to this article or journal.

Reprints and Subscriptions To order reprints of this article or to subscribe to the journal, contact the AACR Publications Department at pubs@aacr.org.

Permissions To request permission to re-use all or part of this article, use this link
<http://cancerimmunolres.aacrjournals.org/content/3/8/849>.
Click on "Request Permissions" which will take you to the Copyright Clearance Center's (CCC) Rightslink site.